Calculation of radiation force and torque exerted on a uniaxial anisotropic sphere by an incident Gaussian beam with arbitrary propagation and polarization directions

Zheng-Jun Li,[1,2] Zhen-Sen Wu,[1,*] Qing-Chao Shang,[1] Lu Bai,[1] and Chun-Hui Cao[1]

[1]*School of Science, Xidian University, Xi'an 710071, China*
[2]*lizhengjuncosabc@yahoo.com.cn*
**wuzhs@mail.xidian.edu.cn*

Abstract: On the basis of spherical vector wave functions and coordinate rotation theory, the expansion of the fields of an incident Gaussian beam with arbitrary propagation and polarization directions in terms of spherical vector wave functions is investigated, and beam shape coefficients are derived. Using the results of electromagnetic scattering by a uniaxial anisotropic sphere, the analytical expressions of the radiation force and torque exerted on a homogeneous absorbing uniaxial anisotropic sphere by the arbitrary incident Gaussian beam. We numerically analyze and discuss the following: the effects of an anisotropic absorbing dielectric on the axial and transverse radiation forces exerted by an off-axis Gaussian beam on a uniaxial anisotropic sphere; the variations in the axial, transverse, and resultant radiation forces (with incident angle β and polarization angle α) imposed by an obliquely Gaussian beam on a uniaxial anisotropic sphere; and the results on the characteristics of the three components of the radiation forces versus the center-to-center distance between the sphere and beam. Selected numerically results on the radiation torque exerted on a stationary uniaxial anisotropic transparent or absorbing sphere by a linearly polarized Gaussian beam are shown, and the results are compared with those exerted an isotropic sphere. The accuracy of the theory and code is confirmed by comparing the axial radiation forces with the results obtained from references.

OCIS codes: (290.5850) Scattering, particles; (140.0140) Lasers and laser optics; (160.1190) Anisotropic optical materials.

References and links

1. A. Ashkin, "Acceleration and trapping of particles by radiation pressure," Phys. Rev. Lett. **24**(4), 156–159 (1970).
2. A. Ashkin, "Applications of laser radiation pressure," Science **210**(4474), 1081–1088 (1980).
3. A. Ashkin, J. M. Dziedzic, J. E. Bjorkholm, and S. Chu, "Observation of a single-beam gradient force optical trap for dielectric particles," Opt. Lett. **11**(5), 288–290 (1986).
4. Y. Harada and T. Asakura, "Radiation forces on a dielectric sphere in the Rayleigh scattering regime," Opt. Commun. **124**(5-6), 529–541 (1996).
5. P. C. Chaumet and M. Nieto-Vesperinas, "Time-averaged total force on a dipolar sphere in an electromagnetic field," Opt. Lett. **25**(15), 1065–1067 (2000).
6. A. Rohrbach and E. H. K. Stelzer, "Optical trapping of dielectric particle in arbitrary fields," J. Opt. Soc. Am. A **18**(4), 839–853 (2001).
7. T. C. B. Schut, G. Hesselink, B. G. de Grooth, and J. Greve, "Experimental and theoretical investigations on the validity of the geometrical optics model for calculating the stability of optical traps," Cytometry **12**(6), 479–485 (1991).
8. A. Ashkin, "Forces of a single-beam gradient laser trap on a dielectric sphere in the ray optics regime," Biophys. J. **61**(2), 569–582 (1992).
9. R. Gussgard, T. Lindmo, and I. Brevik, "Calculation of the trapping force in a strongly focused laser beam," J. Opt. Soc. Am. B **9**(10), 1922–1930 (1992).

#166959 - $15.00 USD Received 18 Apr 2012; revised 8 Jun 2012; accepted 22 Jun 2012; published 5 Jul 2012

10. R. C. Gauthier and S. Wallace, "Optical levitation of spheres: analytical development and numerical computations of force equations," J. Opt. Soc. Am. B **12**(9), 1680–1687 (1995).
11. T. Wohland, A. Rosin, and E. H. K. Stelzer, "Theoretical determination of the influence of the polarization on forces exerted by optical tweezers," Optik (Stuttg.) **102**(4), 181–190 (1996).
12. S. Nemoto and H. Togo, "Axial force acting on a dielectric sphere in a focused laser beam," Appl. Opt. **37**(27), 6386–6394 (1998).
13. J. S. Kim and S. S. Lee, "Scattering of laser beams and the optical potential well for a homogeneous sphere," J. Opt. Soc. Am. **73**(3), 303–312 (1983).
14. J. P. Barton, D. R. Alexander, and S. A. Schaub, "Internal and near-surface electromagnetic fields for a spherical particle irradiated by a focused laser beam," J. Appl. Phys. **64**(4), 1632–1639 (1988).
15. J. P. Barton, D. R. Alexander, and S. A. Schaub, "Theoretical determination of net radiation force and torque for a spherical particle illuminated by a focused laser beam," J. Appl. Phys. **66**(10), 4594–4962 (1989).
16. G. Gouesbet, B. Maheu, and G. Grehan, "Light Scattering from a sphere arbitrarily located in a Gaussian beam,using a Bromwich formulation," J. Opt. Soc. Am. A **5**(9), 1427–1443 (1988).
17. G. Gouesbet, G. Gréhan, and B. Maheu, "Localized interpretation to compute all the coefficients gmn in the generalized Lorentz-Mie theory," J. Opt. Soc. Am. A **7**(6), 998–1007 (1990).
18. K. F. Ren, G. Gréha, and G. Gouesbet, "Radiation pressure forces exerted on a particle arbitrarily located in a Gaussian beam by using the generalized Lorenz-Mie theory and associated resonance effects," Opt. Commun. **108**(4-6), 343–354 (1994).
19. K. F. Ren, G. Gréhan, and G. Gouesbet, "Prediction of reverse radiation pressure by generalized Lorenz-Mie theory," Appl. Opt. **35**(15), 2702–2710 (1996).
20. J. A. Lock, "Calculation of the radiation trapping force for laser tweezers by use of generalized Lorenz-Mie theory. I. Localized model description of an on-axis tightly focused laser beam with spherical aberration," Appl. Opt. **43**(12), 2532–2544 (2004).
21. Y. K. Nahmias and D. J. Odde, "Analysis of Radiation Forces in Laser Trapping and Laser-Guided Direct Writing Applications," IEEE J. Quantum Electron. **38**(2), 131–141 (2002).
22. G. Martinot-Lagarde, B. Pouligny, M. I. Angelova, G. Grehan, and G. Gouesbet, "Trapping and levitation of a dielectric sphere with off-centred Gaussian beams. II. GLMT analysis," Pure Appl. Opt. **4**(5), 571–585 (1995).
23. Y. K. Nahmias, B. Z. Gao, and D. J. Odde, "Dimensionless parameters for the design of optical traps and laser guidance systems," Appl. Opt. **43**(20), 3999–4006 (2004).
24. F. L. Mao, Q. R. Xing, K. Wang, L. Y. Lang, L. Chai, and Q. Y. Wang, "Calculation of axial optical forces exerted on medium-sized particles by optical trap," Opt. Laser Technol. **39**(1), 34–39 (2007).
25. R. D. Graglia and P. L. E. Uslenghi, "Electromagnetic Scattering from Anisotropic Materials, Part I: General Theory," IEEE Trans. Antenn. Propag. **32**(8), 867–869 (1984).
26. S. N. Papadakis, N. K. Uzunoglu, and C. N. Capsalis, "Scattering of a plane wave by a general anisotropic dielectric ellipsoid," J. Opt. Soc. Am. A **7**(6), 991–997 (1990).
27. W. Ren, "Contributions to the electromagnetic wave theory of bounded homogeneous anisotropic media," Phys. Rev. E Stat. Phys. Plasmas Fluids Relat. Interdiscip. Topics **47**(1), 664–673 (1993).
28. J. A. Pereda, L. A. Vielva, A. Vegas, and A. Prieto, "FDTD Analysis of Magnetized Ferrites: Application to the Calculation of Dispersion Characteristics of Ferrite-Loaded Waveguides," IEEE Trans. Antenn. Propag. **43**(2), 350–357 (1995).
29. S. C. Mao, Z. S. Wu, and H.-Y. Li, "Three-dimensional scattering by an infinite homogeneous anisotropic elliptic cylinder in terms of Mathieu functions," J. Opt. Soc. Am. A **26**(11), 2282–2291 (2009).
30. Y. L. Geng, X. B. Wu, L. W. Li, and B. R. Guan, "Mie scattering by a uniaxial anisotropic sphere," Phys. Rev. E Stat. Nonlin. Soft Matter Phys. **70**(5), 056609 (2004).
31. B. Stout, M. Nevière, and E. Popov, "Mie scattering by an anisotropic object. Part I. Homogeneous sphere," J. Opt. Soc. Am. A **23**(5), 1111–1123 (2006).
32. C. W. Qiu, S. Zouhdi, and A. Razek, "Modified Spherical Wave Functions With Anisotropy Ratio: Application to the Analysis of Scattering by Multilayered Anisotropic Shells," IEEE Trans. Antenn. Propag. **55**(12), 3515–3523 (2007).
33. M. Sluijter, D. K. G. de Boer, and J. J. M. Braat, "General polarized ray-tracing method for inhomogeneous uniaxially anisotropic media," J. Opt. Soc. Am. A **25**(6), 1260–1273 (2008).
34. Z. S. Wu, Q. K. Yuan, Y. Peng, and Z. J. Li, "Internal and external electromagnetic fields for on-axis Gaussian beam scattering from a uniaxial anisotropic sphere," J. Opt. Soc. Am. A **26**(8), 1778–1788 (2009).
35. Q. K. Yuan, Z. S. Wu, and Z. J. Li, "Electromagnetic scattering for a uniaxial anisotropic sphere in an off-axis obliquely incident Gaussian beam," J. Opt. Soc. Am. A **27**(6), 1457–1465 (2010).
36. Z. J. Li, Z. S. Wu, and Q. C. Shang, "Calculation of radiation forces exerted on a uniaxial anisotropic sphere by an off-axis incident Gaussian beam," Opt. Express **19**(17), 16044–16057 (2011).
37. S. Chang and S. S. Lee, "Optical torque exerted on a homogeneous sphere levitated in the circularly polarized fundamental-mode laser beam," J. Opt. Soc. Am. B **2**(11), 1853–1860 (1985).
38. F. Xu, J. Lock, G. Gouesbet, and C. Tropea, "Radiation torque exerted on a spheroid: Analytical solution," Phys. Rev. A **78**(1), 013843 (2008).
39. G. Gouesbet, "T-matrix formulation and generalized lozrenz-Mie theories in spherical coordinates," Opt. Commun. **283**(4), 517–521 (2010).
40. G. Gouesbet and J. A. Lock, "Rigorous justification of the localized approximation to the beam-shape coefficients in generalized Lorenz-Mie theory. II. off-axis beams," J. Opt. Soc. Am. A **11**(9), 2516–2525 (1994).

#166959 - $15.00 USD Received 18 Apr 2012; revised 8 Jun 2012; accepted 22 Jun 2012; published 5 Jul 2012

41. A. Doicu and T. Wriedt, "Computation of the beam-shape coefficients in the generalized Lorenz-Mie theory by using the translational addition theorem for spherical vector wave functions," Appl. Opt. **36**(13), 2971–2978 (1997).
42. Y. P. Han, H. Y. Zhang, and G. X. Han, "The expansion coefficients of arbitrary shaped beam in oblique illumination," Opt. Express **15**(2), 735–746 (2007).
43. G. Gouesbet, J. J. Wang, and Y. P. Han, "Transformations of spherical beam shape coefficients in generalized Lorenz-Mie theories through rotations of coordinate systems," Opt. Commun. **283**(17), 3218–3225 (2010).

1. Introduction

Since the pioneering work of Ashkin and associates [1–3], optical tweezers have attracted considerable attention and have been extensively applied in various fields. In principle, small particles (e.g., biological cells) with micrometer and sub-micrometer dimensions can be trapped and non-intrusively manipulated under the radiation force (RF) generated by tightly focused laser beams. Researchers have used various methods to compute the RF exerted on homogeneous isotropic spherical particles. For a particle much smaller than the incident wavelength ($d << \lambda$), the Rayleigh regime is considered, and RF can be calculated by Rayleigh dipole approximation (RDA) [4, 5]. By expanding the incident field into a plane wave spectrum, Rohrbach et al. [6] extended the validity range of Rayleigh theory to particle sizes as large ~0.7λ. Conversely, for a particle much larger than the incident wavelength (typically $d / \lambda > 10$), the geometrical optics regime is considered; in this case, ray optics theory (ROT) is a highly applicable and efficient approach to calculating RF [7–12]. For a particle whose size is of incident wavelength order, both RDA and ROT are inapplicable because diffraction phenomena cannot be neglected in this case. To cover the entire d/λ range, a rigorous electromagnetic theory has been developed for a spherical particle interacting with a laser beam. In this theory, expanding an incident beam in terms of spherical vector wave functions (SVWFs) is necessary. Kim and Lee [13] used the complex-source-point method to expand the incident field components of Hermite–Gaussian laser beams, and calculated the optical potential well exerted on a homogeneous sphere. Using the surface integral method, Barton expanded the incident field components of a Gaussian beam [14] and studied the net RF and torque for a spherical particle [15]. Gouesbet et al. [16] proposed generalized Lorez-Mie theory (GLMT), which employs a set of beam shape coefficients to describe the incident beam [17]. Applying GLMT, Ren et al. [18, 19], Lock et al. [20], Nahmias et al. [21], and Martinot-Lagarde et al. [22] investigated the RF exerted on a spherical particle. Nahmias et al. [23] and Mao et al. [24] compared the RFs obtained by ROT and GLMT, and described the limitations of ROT, which confirm that GLMT is a complete beam-scattering theory for particles of all sizes.

Compared with studies on RF calculations for isotropic spherical particles, those devoted to RF prediction for anisotropic particles are considerably rare. Anisotropic medium has drawn increasing attention because of their wide applicability in optical signal processing, and microwave engineering, and so on. In past decades, many scholars have studied the interaction of a plane wave with anisotropic particles [25–29], especially with uniaxial anisotropic spherical particles [30–33]. Researchers from our group recently studied the scattering characteristic of a uniaxial anisotropic sphere illuminated by on-axis, off-axis, and arbitrarily incident Gaussian beams, and discussed the scattered, internal, and incident fields [34, 35]. The RF exerted on an anisotropic sphere may represent varied properties because of the differences in the internal fields of anisotropic and isotropic spheres. Thus, the RF exerted by a focused laser beam on an anisotropic spherical particle is also a critical and interesting study object. The authors have recently investigated the RF exerted by an off-axis Gaussian beam on a uniaxial anisotropic sphere [36]. Since that a uniaxial anisotropic sphere has a primary optical axis, the internal and scattered fields created when the beam's propagation direction is not parallel to the primary optical axis of the anisotropic sphere will be distinct from the fields created when the beam's propagation direction is parallel to the primary optical axis. Thus, the RF exhibits different characteristics. Prediction of the RF exerted by an off-axis obliquely incident Gaussian beam on a uniaxial anisotropic sphere is still in its infancy, but is an endeavor of considerable merit. Comparing the RF, the performance the

#166959 - $15.00 USD Received 18 Apr 2012; revised 8 Jun 2012; accepted 22 Jun 2012; published 5 Jul 2012

radiation torque causes rotation of a particle is also very useful and interesting phenomenon. Chang and Lee [37] and Barton [15] studied the radiation torque exerted on an isotropic sphere by a linearly and circular polarized Gaussian beam. Xu [38] investigated radiation torque exerted on a spheroid by a Gaussian beam. Because the internal field is made up of two EM waves with different velocities and polarization directions, the radiation torque exerted on a uniaxial anisotropic sphere by an arbitrary direction incident Gaussian beam will be not always zero like that exerted on an isotropic sphere. Thus, it is worthy to research this problem which is still solved.

In this paper, based on the GLMT [16] and coordinate rotation theory of SVWFs the field components of an incident Gaussian beam with arbitrary propagation and polarization directions are expanded in terms of SVWFs in a fixed rectangular coordinate system. According to the orthogonality of associated Legendre functions and trigonometric functions, we derive the analytical expressions of the transverse and axial RFs and radiation torque exerted on a uniaxial anisotropic sphere in the incident Gaussian beam. Numerical calculations of the radiation force and torque are carried out, and their physical interpretations are presented.

In the subsequent depiction, a time dependence of the form $\exp(-i\omega t)$ is assumed and suppressed, where ω is the circular frequency.

2. Theory

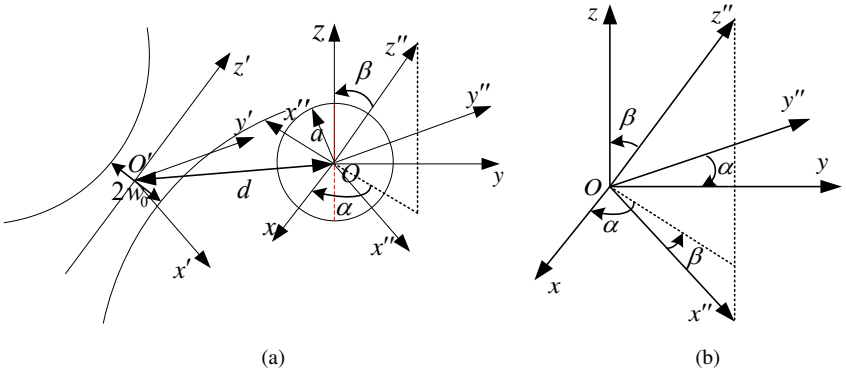

(a) (b)

Fig. 1. (a) Uniaxial anisotropic sphere is illuminated by an incident Gaussian beam with arbitrary directions of propagation and polarization. (b) Rotation relationships of two coordinate system.

Consider a homogeneous uniaxial anisotropic sphere of radius a centrally located in a spherical coordinate system. The primary optical axis is coincident with the z-axis. As Fig. 1(a) shows, the particle is obliquely illuminated by an x'-polarized Gaussian beam that propagates in the z'-direction in Cartesian coordinate system $O'x'y'z'$, with the beam center located at O'. The coordinates of beam center O' are (x_0, y_0, z_0) in $Oxyz$. Temporary coordinate system $Ox"y"z"$ is established parallel to $O'x'y'z'$ and is known as the beam system. We denote the propagation direction of the beam as two angles in particle coordinate system $Oxyz$; that is, incident angle β with reference to the z-axis, and polarization angle α between the x-axis and the propagation direction of the beam on the xoy-plane. Then, $Oxyz$ can be obtained by rotating $Ox"y"z"$ with Euler angles β and α (Fig. 1(b)).

2.1. Description of the incident and scattered fields

In terms of SVWFs, the incident Gaussian beam can be expanded in temporary coordinate system $Ox"y"z"$ as follows [39]:

#166959 - $15.00 USD Received 18 Apr 2012; revised 8 Jun 2012; accepted 22 Jun 2012; published 5 Jul 2012

$$\mathbf{E}^{i''} = E_0 \sum_{n=1}^{\infty} \sum_{m=-n}^{n} \left[i g_{n,TE}^{m}{}'' \mathbf{M}_{mn}^{(1)}(\mathbf{r}'', k_0) + g_{n,TM}^{m}{}'' \mathbf{N}_{mn}^{(1)}(\mathbf{r}'', k_0) \right],$$
$$\mathbf{H}^{i''} = E_0 \frac{k_0}{\omega \mu_0} \sum_{n=1}^{\infty} \sum_{m=-n}^{n} \left[g_{n,TE}^{m}{}'' \mathbf{N}_{mn}^{(1)}(\mathbf{r}'', k_0) - i g_{n,TM}^{m}{}'' \mathbf{M}_{mn}^{(1)}(\mathbf{r}'', k_0) \right], \quad (1)$$

Here, $k_0 = 2\pi/\lambda$ and λ is a surrounding medium wavelength, μ_0 denotes the permeability of the surrounding medium, and E_0 is the amplitude of the electric field at the beam center. SVWFs $\mathbf{M}_{mn}^{(l)}(\mathbf{r}, k)$ and $\mathbf{N}_{mn}^{(l)}(\mathbf{r}, k)$ can be found in [34]. $g_{n,TE}^{m}{}''$ and $g_{n,TM}^{m}{}''$ are the beam shape coefficients obtained by applying the local approximation of GLMT in beam system $Ox''y''z''$ [40, 41]:

$$\begin{bmatrix} g_{n,TM}^{m}{}'' \\ i g_{n,TE}^{m}{}'' \end{bmatrix} = (-1)^{m-1} C_{nm} K_{nm} \psi_0'' e^{ik_0 z_0''} \frac{1}{2} \left[e^{i(m-1)\varphi_0''} J_{m-1}(2\frac{\bar{Q}_0'' \rho_0'' \rho_n}{w_0^2}) \pm e^{i(m+1)\varphi_0''} J_{m+1}(2\frac{\bar{Q}_0'' \rho_0'' \rho_n}{w_0^2}) \right], \quad (2)$$

where

$$\psi_0'' = i\bar{Q}_0'' \exp(-i\bar{Q}_0'' \rho_0''^2 / w_0^2) \exp(-i\bar{Q}_0''(n+0.5)^2 / k_0^2 w_0^2),\ \bar{Q}_0'' = (i - 2z_0'' / (k_0 w_0^2))^{-1}$$
$$\rho_0'' = \sqrt{x_0''^2 + y_0''^2}, \rho_n = (n+0.5)/k_0, \varphi_0'' = \arctan(x_0'' / y_0''), \quad (3)$$

$$C_{nm} = \begin{cases} i^{n-1} \dfrac{2n+1}{n(n+1)}, & m \geq 0 \\ (-1)^{|m|} \dfrac{(n+|m|)!}{(n-|m|)!} i^{n-1} \dfrac{2n+1}{n(n+1)}, & m < 0 \end{cases}, \quad K_{nm} = \begin{cases} (-i)^{|m|} \dfrac{i}{(n+0.5)^{|m|-1}}, & m \neq 0 \\ \dfrac{n(n+1)}{n+0.5}, & m = 0 \end{cases}. \quad (4)$$

In the above-mentioned equations, w_0 is the beam waist radius, and (x_0", y_0", z_0") are the coordinates of beam center O' in $Ox"y"z"$. According to the coordinate rotation relationship, (x_0", y_0", z_0") can be derived from (x_0, y_0, z_0) by:

$$\begin{pmatrix} x_0'' \\ y_0'' \\ z_0'' \end{pmatrix} = \begin{pmatrix} \cos\beta & 0 & \sin\beta \\ 0 & 1 & 0 \\ -\sin\beta & 0 & \cos\beta \end{pmatrix} \begin{pmatrix} \cos\alpha & \sin\alpha & 0 \\ -\sin\alpha & \cos\alpha & 0 \\ 0 & 0 & 1 \end{pmatrix} \begin{pmatrix} x_0 \\ y_0 \\ z_0 \end{pmatrix}. \quad (5)$$

For two coordinate systems $Oxyz$ and $Ox"y"z"$, with a rotation relationship determined by Euler angles β and α, the SVWFs have the following relationships [35, 42, 43]:

$$(\mathbf{M}, \mathbf{N})_{mn}^{(1)}(\mathbf{r}'', k_0) = \sum_{s=-n}^{n} \rho(m, s, n) (\mathbf{M}, \mathbf{N})_{sn}^{(1)}(\mathbf{r}, k_0), \quad (6)$$

where

$$\rho(m, s, n) = (-1)^{s+m} e^{-is\alpha} [\frac{(n+m)!(n-s)!}{(n-m)!(n+s)!}]^{1/2} \mathrm{u}_{sm}^{(n)}(-\beta), \quad (7)$$

#166959 - $15.00 USD Received 18 Apr 2012; revised 8 Jun 2012; accepted 22 Jun 2012; published 5 Jul 2012

$$\mathrm{u}_{sm}^{(n)}(-\beta)=\left[\frac{(n+s)!(n-s)!}{(n+m)!(n-m)!}\right]^{1/2}\sum_{\sigma}\binom{n+m}{n-s-\sigma}\binom{n-m}{\sigma}(-1)^{n-s-\sigma}(\cos\frac{-\beta}{2})^{2\sigma+s+m}(\sin\frac{-\beta}{2})^{2n-2\sigma-s-m}. \tag{8}$$

Coefficient $\rho(m,s,n)$ slightly differs from that described in [35, 42, 43] because the current study adopts the anti-clockwise rotation of the two coordinate systems, whereas in [35, 42, 43] the clockwise relationship is employed. Moreover, we use only Euler angles α and β to denotes that the incident direction of the Gaussian beam is arbitrary; that is, arbitrarily incident and polarization-oriented β and α, respectively. This depiction not only maintains generality, but also enables the simplification of the problem compared with the depiction in [35]. Substituting Eq. (6) into Eq. (1), we derive the expanded form of the incident field in particle coordinate system *Oxyz*:

$$\begin{aligned}\mathbf{E}^i&=E_0\sum_{n=1}^{\infty}\sum_{m=-n}^{n}\left[a_{mn}^i\mathbf{M}_{mn}^{(1)}(\mathbf{r},k_0)+b_{mn}^i\mathbf{N}_{mn}^{(1)}(\mathbf{r},k_0)\right],\\ \mathbf{H}^i&=E_0\frac{k_0}{i\omega\mu_0}\sum_{n=1}^{\infty}\sum_{m=-n}^{n}\left[a_{mn}^i\mathbf{N}_{mn}^{(1)}(\mathbf{r},k_0)+b_{mn}^i\mathbf{M}_{mn}^{(1)}(\mathbf{r},k_0)\right],\end{aligned} \tag{9}$$

where

$$\left(a_{mn}^i,b_{mn}^i\right)=\sum_{s=-n}^{n}\rho(s,m,n)C_{ns}\left(ig_{n,TE}^{\prime\prime s},g_{n,TM}^{\prime\prime s}\right). \tag{10}$$

and $\rho(s,m,n)$ can be obtained by interchanging *m* with *s* in Eq. (7).

The scattered fields can be expanded with the SVWFs as follows:

$$\begin{aligned}\mathbf{E}^s&=E_0\sum_{n=1}^{\infty}\sum_{m=-n}^{n}[A_{mn}^s\mathbf{M}_{mn}^{(3)}(\mathbf{r},k_0)+B_{mn}^s\mathbf{N}_{mn}^{(3)}(\mathbf{r},k_0)],\\ \mathbf{H}^s&=E_0\frac{k_0}{i\omega\mu}\sum_{n=1}^{\infty}\sum_{m=-n}^{n}[A_{mn}^s\mathbf{N}_{mn}^{(3)}(\mathbf{r},k_0)+B_{mn}^s\mathbf{M}_{mn}^{(3)}(\mathbf{r},k_0)].\end{aligned} \tag{11}$$

For a uniaxial anisotropic sphere whose permittivity and permeability tensors $\overline{\varepsilon}$ and $\overline{\mu}$ are characterized by

$$\overline{\varepsilon}=\begin{bmatrix}\varepsilon_t&0&0\\0&\varepsilon_t&0\\0&0&\varepsilon_z\end{bmatrix},\quad \overline{\mu}=\begin{bmatrix}\mu_t&0&0\\0&\mu_t&0\\0&0&\mu_z\end{bmatrix}. \tag{12}$$

the internal fields can be expanded in terms of the SVWFs using Fourier transform [30, 34, 35]. Utilizing the continuity of the tangential electric and magnetic field components at $r = a$, the scattering coefficients can be obtained thus [30, 34]:

$$A_{mn}^s=\frac{1}{h_n^{(1)}(k_0a)}\left[\sum_{n'=1}^{\infty}2\pi G_{mn'q}\sum_{q=1}^{2}\int_0^{\pi}A_{mnq}^e j_n(k_qa)P_{n'}^m(\cos\theta_k)k_q^2\sin\theta_k d\theta_k-a_{mn}^i j_n(k_0a)\right], \tag{13}$$

$$B_{mn}^s=\frac{1}{h_n^{(1)}(k_0a)}\left[\frac{i\omega\mu}{k_0}\sum_{q=1}^{2}\sum_{n'=1}^{\infty}2\pi G_{mn'q}\int_0^{\pi}A_{mnq}^h j_n(k_qa)P_{n'}^m(\cos\theta_k)k_q^2\sin\theta_k d\theta_k-b_{mn}^i j_n(k_0a)\right]. \tag{14}$$

#166959 - $15.00 USD Received 18 Apr 2012; revised 8 Jun 2012; accepted 22 Jun 2012; published 5 Jul 2012

The solution of unknown expansion coefficient $G_{mn'q}$ can be found in [35]. The expressions of coefficients A^{e}_{mnq}, B^{e}_{mnq}, C^{e}_{mnq}, A^{h}_{mnq}, B^{h}_{mnq}, and C^{h}_{mnq} are detailed in [30].

2.2. Derivation of radiation force

Assuming a steady-state condition, the RF exerted by the beam on the particle is proportional to the net momentum removed from the incident beam. It can be expressed as a close spherical surface integral surrounding particle [15]:

$$\mathbf{F}=\frac{1}{2}\mathrm{Re}\int_0^{2\pi}\int_0^{\pi}\left[\varepsilon E_r\mathbf{E}+\mu H_r\mathbf{H}-\frac{1}{2}(\varepsilon_0E^2+\mu_0H^2)\hat{e}_r\right]r^2\sin\theta\,d\theta\,d\phi\Big|_{r>a}. \quad (15)$$

where ε and μ are the permittivity and permeability of the surrounding medium, respectively. The EM fields indicate the superposition of the incident and scattered EM fields: $\mathbf{E}=\mathbf{E}^i+\mathbf{E}^s$, $\mathbf{H}=\mathbf{H}^i+\mathbf{H}^s$.

Scattering theory indicates that for spherical particles, the axial components of the incident and scattering fields are very small and can be negligible in the far region. Then, the RF can be written as:

$$\begin{aligned}\mathbf{F}=&-\frac{1}{2}\mathrm{Re}\int_0^{2\pi}\int_0^{\pi}\frac{1}{2}[\varepsilon(E^i_\theta E^{i*}_\theta+E^i_\theta E^{s*}_\theta+E^s_\theta E^{i*}_\theta+E^s_\theta E^{s*}_\theta+E^i_\phi E^{i*}_\phi+E^i_\phi E^{s*}_\phi+E^s_\phi E^{i*}_\phi+E^s_\phi E^{s*}_\phi)\\&+\mu(H^i_\theta H^{i*}_\theta+H^i_\theta H^{s*}_\theta+H^s_\theta H^{i*}_\theta+H^s_\theta H^{s*}_\theta+H^i_\phi H^{i*}_\phi+H^i_\phi H^{s*}_\phi+H^s_\phi H^{inc*}_\phi+H^s_\phi H^{s*}_\phi)]r^2\sin\theta\,d\theta\,d\phi\Big|_{r>a}.\end{aligned} \quad (16)$$

The numerical calculation of the surface integral of Eq. (16) can be avoided by substituting the series expressions for electromagnetic field components and using the approximate expressions of Ricatti-Bessel functions at $r\gg\lambda$:

$$\xi_n(kr)\to(-i)^{n+1}\exp(ikr), \quad (17)$$

After substantial algebraic computation and application of the numerous recursion, product, and orthogonality relationships of associated Legendre functions and trigonometric functions, Eq. (16) can be directly integrated, and the net force on the particle can be expressed as a series over the expansion coefficients of the incident and scattered fields [36]:

$$\begin{aligned}F_x+iF_y=&\frac{4n_0P_0}{ck_0^2w_0^2}\sum_{n=1}^{\infty}\sum_{m=-n}^{n}[\frac{(n+m+1)!}{(2n+1)(n-m-1)!}(a^i_{mn}B^{s*}_{m+1n}+b^i_{mn}A^{s*}_{m+1n}+B^s_{mn}a^{i*}_{m+1n}+A^s_{mn}b^{i*}_{m+1n}\\&+2A^s_{mn}B^{s*}_{m+1n}+2B^s_{mn}A^{s*}_{m+1n})-\frac{i(n-1)(n+1)(n+m)!}{(2n-1)(2n+1)(n-m-2)!}N^{-1}_{mn}N^{-1}_{m+1n-1}(a^i_{mn}A^{s*}_{m+1n-1}+b^i_{mn}B^{s*}_{m+1n-1}\\&+A^s_{mn}a^{i*}_{m+1n-1}+B^s_{mn}b^{i*}_{m+1n-1}+2A^s_{mn}A^{s*}_{m+1n-1}+2B^s_{mn}B^{s*}_{m+1n-1})-\frac{in(n+2)(n+m+2)!}{(2n+1)(2n+3)(n-m)!}(a^i_{mn}A^{s*}_{m+1n+1}\\&+b^i_{mn}B^{s*}_{m+1n+1}+A^s_{mn}a^{i*}_{m+1n+1}+B^s_{mn}b^{i*}_{m+1n+1}+2A^s_{mn}A^{s*}_{m+1n+1}+2B^s_{mn}B^{s*}_{m+1n+1})],\end{aligned} \quad (18)$$

$$\begin{aligned}F_z=&\frac{8n_0P_0}{ck_0^2w_0^2}\mathrm{Re}\sum_{n=1}^{\infty}\sum_{m=-n}^{n}[i\frac{n(n+2)(n+m+1)!}{(2n+1)(2n+3)(n-m)!}(a^i_{mn+1}A^{s*}_{mn}+A^s_{mn+1}a^{i*}_{mn}+b^i_{mn+1}B^{s*}_{mn}\\&+B^s_{mn+1}b^{i*}_{mn}+2A^s_{mn+1}A^{s*}_{mn}+2B^s_{mn+1}B^{s*}_{mn})-\frac{m(n+m)!}{(2n+1)(n-m)!}(a^i_{mn}B^{s*}_{mn}+b^i_{mn}A^{s*}_{mn}+2A^s_{mn}B^{s*}_{mn})].\end{aligned} \quad (19)$$

#166959 - $15.00 USD Received 18 Apr 2012; revised 8 Jun 2012; accepted 22 Jun 2012; published 5 Jul 2012

where c is the speed of light in vacuum, n_0 represents the refractive index of the surrounding medium, $P_0 = k_0 \pi w_0^2 E_0^{\ 2} / (4\omega\mu_0)$ denotes the power of the incident beam.

2.3. Derivation of radiation torque

In view of the conservation law of angular momentum, the radiation torque exerted on a uniaxial anisotropic spherical particle equals the average rate at which the angular momentum is transported into the particle. For a steady-state scattering problem, it can be expressed as an integral through the spherical surface centered at the center of the uniaxial anisotropic sphere [15, 37, 38]:

$$\mathbf{T} = -\frac{1}{2}\mathrm{Re}\left\langle \oint_S \hat{n}\cdot([\varepsilon \mathbf{E}\mathbf{E}^* + \mu \mathbf{H}\mathbf{H}^* - \frac{1}{2}\varepsilon |E|^2 \ddot{\mathbf{I}} - \frac{1}{2}\mu |H|^2 \ddot{\mathbf{I}}]\times \mathbf{r})dS \right\rangle, \tag{20}$$

where $\hat{n}$ is the unit vector normal to the surface; $\ddot{\mathbf{I}}$ is the unit dyad tensor; and $\mathbf{r}$ is the distance vector from the origin to the enclosing surface. If the spherical surface of radius $r>a$ is chosen, then,

$$\mathbf{T} = -\frac{1}{2}\mathrm{Re}\int_0^{2\pi}\int_0^{\pi}[(\varepsilon_0 E_r E_\phi^* + \mu_0 H_r H_\phi^*)\hat{e}_\theta - (\varepsilon_0 E_r E_\theta^* + \mu_0 H_r H_\theta^*)\hat{e}_\phi]r^3 \sin\theta d\theta d\phi\Big|_{r>a}. \tag{21}$$

Similarly, substituting the incident and scattered fields into the outward EM fields $\mathbf{E} = \mathbf{E}^i + \mathbf{E}^s$, $\mathbf{H} = \mathbf{H}^i + \mathbf{H}^s$, and applying the recursion and orthogonality relationships of associated Legendre functions and asymptotic formulae of spherical Bessel functions [37], the three components of the radiation torque exerted on a uniaxial anisotropic sphere can be derived:

$$\begin{aligned} T_x = \frac{4nP_0}{k_0^3 c w_0^2}\sum_{n=1}^{\infty}\sum_{m=-n}^{n}\frac{n(n+1)}{2n+1}\frac{(n+m+1)!}{(n-m-1)!}\times \mathrm{Re}[&(a_{mn}^i a_{m+1n}^{s*} + b_{mn}^i b_{m+1n}^{s*}) \\ &+ (a_{mn}^s a_{m+1n}^{i*} + b_{mn}^s b_{m+1n}^{i*}) + 2(a_{mn}^s a_{m+1n}^{s*} + b_{mn}^s b_{m+1n}^{s*})], \end{aligned} \tag{22}$$

$$\begin{aligned} T_y = \frac{4nP_0}{k_0^3 c w_0^2}\sum_{n=1}^{\infty}\sum_{m=-n}^{n}\frac{n(n+1)}{2n+1}\frac{(n+m+1)!}{(n-m-1)!}\times \mathrm{Im}[&(a_{mn}^i a_{m+1n}^{s*} + b_{mn}^i b_{m+1n}^{s*}) \\ &+ (a_{mn}^s a_{m+1n}^{i*} + b_{mn}^s b_{m+1n}^{i*}) + 2(a_{mn}^s a_{m+1n}^{s*} + b_{mn}^s b_{m+1n}^{s*})], \end{aligned} \tag{23}$$

$$T_z = -\frac{8nP_0}{ck_0^3 w_0^2}\sum_{n=1}^{\infty}\sum_{m=-n}^{n}\frac{mn(n+1)}{2n+1}\frac{(n+m)!}{(n-m)!}[\mathrm{Re}(a_{mn}^i a_{mn}^{s*} + b_{mn}^i b_{mn}^{s*}) + (|a_{mn}^s|^2 + |b_{mn}^s|^2)]. \tag{24}$$

3. Numerical calculations

On the basis of theory developed in the preceding section, we present our numerical results.

3.1. Validation of theory and codes

We perform two comparisons to verify the accuracy of our theory. The scattering coefficients or scattered fields are calculated and compared with the results obtained from [35] to verify the accuracy of our results. Figure 2 shows the axial RF from our theory, compared with the results in [36] in which the obliquely incident Gaussian beam is reduced to an on-axis incident Gaussian beam. The accuracy of the results in [36] is verified by comparison with the experimental results otained form [7]. It can be found they are in excellent agreement, which confirms the validity of the theory and code in the present paper. $P_0 = 100\mathrm{mW}$, and d denotes the distance of the sphere center from the beam center. The remaining figures possess similar conditions too. Moreover, the curve denoted by "w_0 = 0.4 μm" indicates that the

#166959 - $15.00 USD Received 18 Apr 2012; revised 8 Jun 2012; accepted 22 Jun 2012; published 5 Jul 2012

uniaxial anisotropic spherical particle can be captured by a focused Gaussian beam, similar to an isotropic sphere. The negative RF only indicates that the direction of the RF is negative but does not reflect the magnitude of the RF.

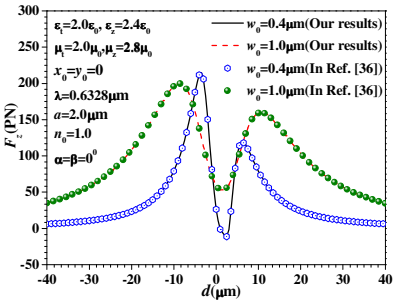

Fig. 2. Comparison of the axial RF from the theory when the obliquely incident Gaussian beam is reduced to an on-axis incident Gaussian beam with the results in reference [36].

3.2. Effects of anisotropic absorbing dielectric

Figures 3(a) and 3(b) shows the variations of the axial RF F_z with d exerted on a uniaxial anisotropic sphere with different complex permittivity tensor elements. "A" and "B" denote the imaginary part of permittivity tensor elements ε_t and ε_z, respectively. It can be found that the influence of the imaginary part of ε_t on the axial RF is more sensitive than that of the imaginary part of ε_z. The same conclusion can be obtained from wave numbers $k_{1,3}^2 = \omega^2\varepsilon_t\mu_t / (\cos^2\theta_k + \mu_t/\mu_z \sin^2\theta_k)$ and $k_{2,4}^2 = \omega^2\varepsilon_t\mu_t / (\cos^2\theta_k + \varepsilon_t/\varepsilon_z \sin^2\theta_k)$ in the uniaxial anisotropic sphere [30]. The influence of ε_t on the wave vectors in the uniaxial anisotropic sphere is larger than that of ε_z. Thus, the influence of ε_t on the scattered field and RF may be more sensitive than that of ε_z. The axial RF increases with the increase of the imaginary part of ε_t when the imaginary part of ε_z is invariable. The axial RF also increases with the increase of the imaginary part of ε_z when the imaginary part of ε_t is invariable. When the imaginary parts of ε_t and ε_z do not equal zero and increase, a great deal of photons are absorbed, thereby rapidly strengthening the scattering force. Thus, the RF quickly increases, so that the particle which can be originally captured is difficult to be captured.

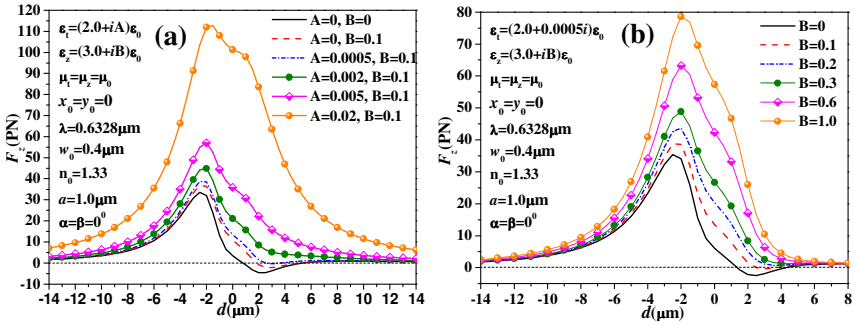

Fig. 3. Effects of absorbing electric anisotropy on axial RF exerted. (a) the imaginary part of ε_t "A" increases. (b) the imaginary part of permittivity tensor elements ε_z "B" increases.

The effects of the absorption of electric anisotropy on the variations of transverse RF F_y with $-x_0$ and F_y with $-y_0$ exerted by an off-axis Gaussian beam on a uniaxial anisotropic sphere are depicted in Fig. 4. The figure also exhibits the same characteristics illustrated in

#166959 - $15.00 USD Received 18 Apr 2012; revised 8 Jun 2012; accepted 22 Jun 2012; published 5 Jul 2012

Fig. 3; that is, the influence of ε_t on the scattered field and RF may be more sensitive than that of ε_z. When the imaginary part of ε_t is large (e.g., A = 0.2 in Figs. 4(a) and 4(b)), the transverse RF only slightly changes provided that the imaginary part of ε_z exhibits a little increase (e.g., B from 0.1 to 0.5 in Figs. 4(a) and 4(b)).

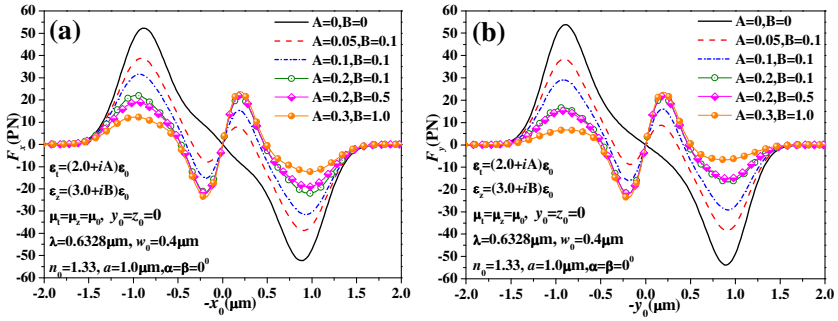

Fig. 4. (a) Effects of absorbing electric anisotropy on transverse RF F_x. (b) Effects of absorbing electric anisotropy on transverse RF F_y.

It can be seen that the uniaxial anisotropic sphere can be bound in the transverse direction when the anisotropic dielectric sphere is lossless. When the anisotropic dielectric sphere is lossy, the secondary extremum of the transverse RF occurs. Moreover, the value of the secondary extremum increases with the increasing imaginary parts of ε_t and ε_z, whereas the peak value of the transverse RF decreases with the increasing imaginary parts of ε_t and ε_z. Thus, when the imaginary parts of ε_t and ε_z are very large, the uniaxial anisotropic sphere may be not bound in the transverse direction (e.g., A = 0.2 and B = 0.5; A = 0.3 and B = 1.0 in Figs. 4(a) and 4(b)). The variations of the transverse RF F_x with $-x_0$ and F_y with $-y_0$ exerted on a uniaxial anisotropic sphere are very similar, since permittivity tensor element ε_t and permeability tensor element μ_t in the *x*-direction and *y*-direction are the same.

3.3. Effects of incident angle and polarization angle

Figure 5(a) shows that the three components of the RF and the resultant RF F_e change with incident angle β exerted on a uniaxial anisotropic sphere under only electric anisotropy. The resultant RF F_e is calculated by $F_e = \sqrt{F_x^2 + F_y^2 + F_z^2}$. The angles are varied only from 0° to 90° to keep the incident orientation under the *xoy*-plane. Transverse RF F_y equals zero because polarization α also equals zero. Axial RF F_z exhibits its maximum value at $\beta = 36°$, and its minimum value at $\beta = 90°$. Note that the minimum is not zero but –0.0742 pN, which results from the effect of ε_z. This characteristic is distinct from that of an isotropic sphere. For an isotropic sphere illuminated by a vertical Gaussian beam, axial RF F_z, which is vertical to the propagation direction of the incident wave, is zero. In Fig. 5(a), transverse RF F_x increases with increasing incident angle, and exhibits its maximum value at of $\beta = 90°$. The resultant RF has the maximum at $\beta = 50°$. Thus, we can conclude that the RF does not remain constant under different incident angles. Figure 5(b) shows the variations of the direction of the resultant RF F_e with the incident angle. θ and ϕ are formed by the direction of the resultant RF with the *z*-axis and *x*-axis, respectively. The azimuth angle is zero because transverse RF F_y equals zero. Both transverse RFs F_x and F_y equal zero when $\beta = 0°$; in Fig. 5(a), therefore, the values of θ and ϕ are not given when $\beta = 0°$. θ is always smaller

#166959 - $15.00 USD Received 18 Apr 2012; revised 8 Jun 2012; accepted 22 Jun 2012; published 5 Jul 2012

than the incident angle of the Gaussian beam. When axial RF F_z is negative, θ is greater than 90°.

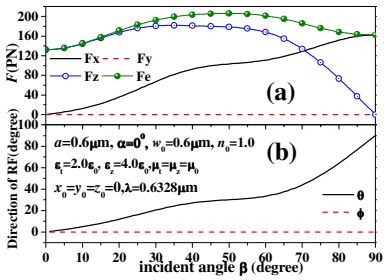

Fig. 5. RF versus the incident angle β. (1) (a) is plotted the three components of the RF and the resultant RF versus β; (2) (b) is plotted the direction of the resultant RF.

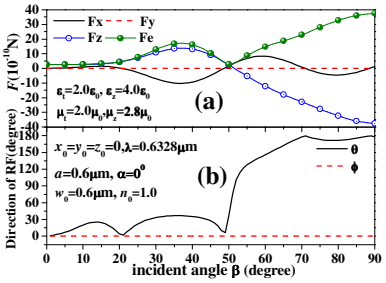

Fig. 6. RF versus the incident angle β. (1) (a) is plotted the three components of the RF and the resultant RF versus β; (2) (b) is plotted the direction of the resultant RF.

Similar to Fig. 5(a), Fig. 6(a) shows the variations of the three components of the RF and the resultant RF F_e with incident angle β exerted on a uniaxial anisotropic sphere with both electric and magnetic anisotropy. The comparison of Figs. 5(a) and 6(a) shows that transverse RF F_x and axial RF F_z are considerably larger when μ_t and μ_z are not equal to μ_0 than those when $\mu_t = \mu_z = \mu_0$. Moreover, the variations with the incident angle are also more complex. Under many incident angles, transverse RF F_x and axial RF F_z are negative. The variations of the direction of the resultant RF F_e with the incident angle are shown in Fig. 6(b). A comparison of Figs. 6(a) with 6(b) indicates that the resultant RF F_e has the maximum value of 3755.4 pN at $\beta = 90°$, and its orientation angle $\theta = 178.135°$. That is, the maximal resultant RF is very large and occurs almost along the $-z$-axis. These properties, which are distinct from those of an isotropic sphere, may pertain only to the uniaxial anisotropic sphere and may be applicable to non-intrusive optical detection of optics material through giving the particle approach the surface of optics material a force vertical to the surface, thereby delivering or capturing the particle. Permittivity tensor elements ε_t and ε_z and permeability tensor elements μ_t and μ_z impose remarkable influence on the variations of the axial and transverse RFs with the incident angle. Thus, the differences in the permittivity tensor elements and permeability tensor elements may cause distinct variations of the RF with the incident angle.

#166959 - $15.00 USD Received 18 Apr 2012; revised 8 Jun 2012; accepted 22 Jun 2012; published 5 Jul 2012

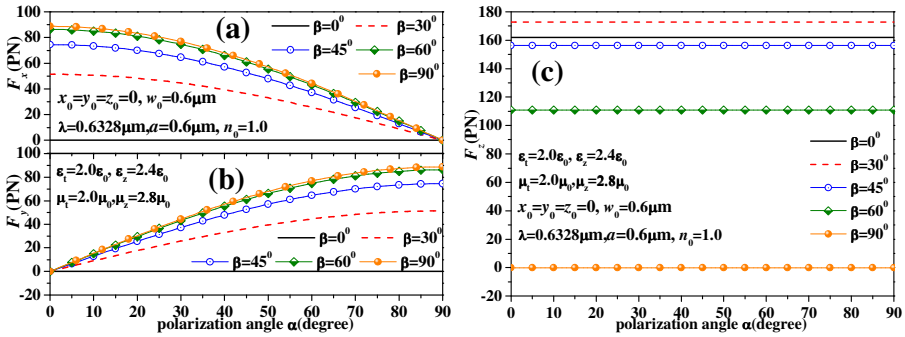

Fig. 7. Variation of RF with polarization angle α for different incident angles β. (a) Transverse RF F_x. (b) Transverse RF F_y. (c) Axial RF F_z.

The three RF components change with polarization angle α for different incident angles β exerted on a uniaxial anisotropic sphere are shown in Fig. 7. Transverse RFs F_x and F_y equal zero when $\beta = 0°$, as expected, and they increase as a whole with increasing incident angle β. However, the shape of the curve exhibits little change. As polarization angle α increases, transverse RF F_x decreases whereas F_y increases. Transverse RFs F_x and F_y yield maximum values at $\beta = 0°$ and $\beta = 90°$, respectively, and exhibit minimum values at $\beta = 90°$ and $\beta = 0°$, respectively. That is, when the incident Gaussian beam is x-axis polarized, F_x has the maximum value but F_y equals zero; when the incident Gaussian beam is y-axis polarized, F_y has the maximum value but F_x equals zero. This phenomenon is highly reasonable. In addition, the variations of the transverse RFs F_x and F_y with the polarization angle are almost oppositely symmetrical. This result may be attributed to the identical permittivity tensor element ε_t and permeability tensor element μ_t along the x-direction and y-direction. Figure 7(c) shows that polarization imposes a minimal effect on axial RF F_z because the change of the polarization angle causes almost no change in scattering along the propagation direction of the incident Gaussian beam. Note that the value of the axial RF when $\beta = 90°$ is not zero but –0.10202 pN. This result is similar to that shown in Figs. 7(a) and 7(c).

TiO_2, characterized by $\varepsilon_t = 5.913\varepsilon_0$ and $\varepsilon_z = 7.197\varepsilon_0$, is a typical uniaxial anisotropic medium. The transverse and axial RF exerted on a TiO_2 sphere by a Gaussian beam with different incident angles as a function of the coordinates of beam center $-x_0$ and $-z_0$ are given in Figs. 8(a) and 8(b), respectively. Transverse RF F_y equals zero because the polarization equals zero (not plotted here). As incident angle β increases, axial RF F_z decreases, whereas transverse RF F_x generally increases as a whole. When $\beta = 0°$, that is, the Gaussian beam propagates along the z-axis, the TiO_2 sphere can be captured in the direction of the x-axis (see the curve denoted by "$F_x(\beta = 0°)$" in Fig. 8(a)). However, the particle will not be captured in the z-axis direction (refer to the curve denoted by "$F_z(\beta = 0°)$" in Fig. 8(b)) because permittivity tensor elements ε_t and ε_z are very large, while the refractive index of the surrounding medium is small. A small beam waist width and large refractive index of the surrounding medium should be selected to capture a uniaxial anisotropic sphere similar to the TiO_2 sphere. The same conclusion is drawn in [36]. When $\beta = 90°$, that is, the Gaussian beam vertically illuminates the TiO_2 sphere, the uniaxial anisotropic sphere can also be captured in the direction of the z-axis (see the curve denoted by "$F_z(\beta = 90°)$" in Fig. 8(b)); it is not captured in the direction of the x-axis (see the curve denoted by "$F_x(\beta = 90°)$" in Fig. 8(a)). When the TiO_2 sphere is illuminated by an absolutely obliquely incident Gaussian beam (e.g., $\beta = 45°$), the TiO_2 sphere is very difficult to capture in both the x-axis and z-axis directions.

#166959 - $15.00 USD Received 18 Apr 2012; revised 8 Jun 2012; accepted 22 Jun 2012; published 5 Jul 2012

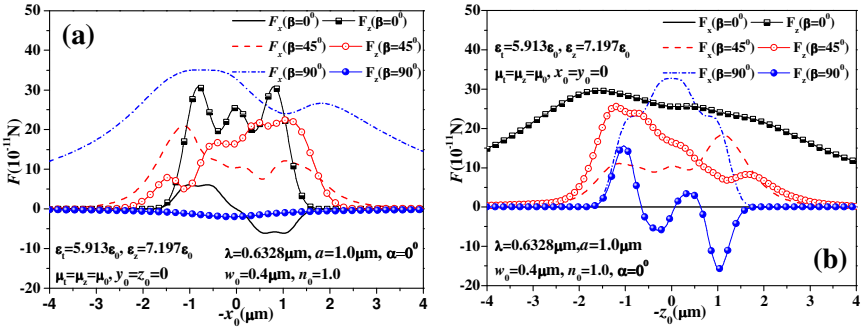

Fig. 8. (a) Variation of RF with $-x_0$ for different incident angle β. (b) Variation of RF with $-z_0$ for different incident angle β.

3.4. Calculation and discussion of radiation torque

In Fig. 9, x component of the radiation torque T_x is calculated when the beam center moves along y-axis. Here, the y and z components of the radiation torque zero due to the symmetry of the spherical particle, and are not plotted in Fig. 9. When $\varepsilon_t = \varepsilon_z$, the anisotropic sphere is reduced to an isotropic sphere. For lossless isotropic sphere, the x component of the radiation torque is always equal to zero, as it should be; while for lossless anisotropic sphere the x component of the radiation torque is not always equal to zero. This is because the internal field consists of two EM waves with different velocities and polarization directions, then the orbital angular momentum may be transferred to the anisotropic particle when propagation direction of the beam is not coincident with the primary optical axis of the anisotropic sphere. This radiation torque will cause the anisotropic to rotate with x-axis, thus, the primary optical axis will be changed so that the scattering field and radiation force will be changed. In this case, it may be difficult to capture the uniaxial anisotropic spherical particle in transverse direction. This performance on radiation force and torque is very different from that of an isotropic spherical particle.

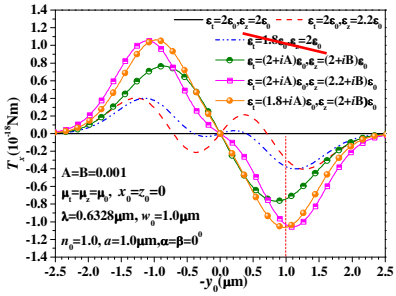

Fig. 9. Torque about z-axis T_x versus the location of the beam center along y axis.

For loss isotropic or anisotropic sphere, the orbital angular momentum may be transferred to the particle through absorption, resulting in an orbital torque. Comparing with lossless uniaxial anisotropic sphere, the radiation torques exerted on a positive($\varepsilon_t<\varepsilon_z$) or negative($\varepsilon_t>\varepsilon_z$) uniaxial anisotropic sphere increase in whole and are larger than those exerted on an lossless anisotropic sphere, and the secondary extremum is also eliminated. As the beam center moves away from the sphere center along y-axis, the lever-arm increases so that the torque increases. When the beam center locates at about the edge of the sphere, the radiation torque procures maxima. The position of the beam center when the maximal radiation torque occurs exerted on an anisotropic sphere is farther from the sphere center than that on an isotropic sphere. Less beam ling flux will incident on the sphere and less angular momentum will be transferred with the increasing of $|y_0|$, thus the radiation torque decreases.

#166959 - $15.00 USD Received 18 Apr 2012; revised 8 Jun 2012; accepted 22 Jun 2012; published 5 Jul 2012

Moreover, it can be found that the radiation torques T_x for both isotropic and anisotropic sphere are zero, as expected. .

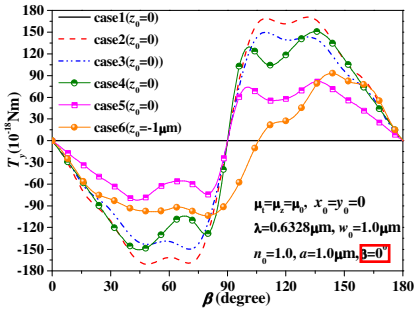

Fig. 10. Torque about y-axis T_y versus the incident angle β, the permittivity and permeability tensors elements are $\varepsilon_t = \varepsilon_z = 2\varepsilon_0$, $\mu_t = \mu_z = 1\mu_0$ in case1; $\varepsilon_t = 2\varepsilon_0$, $\varepsilon_z = 4\varepsilon_0$, $\mu_t = \mu_z = \mu_0$ in case2; $\varepsilon_t = (2 + 0.01i)\varepsilon_0$, $\varepsilon_z = (4 + 0.01i)\varepsilon_0$, $\mu_t = \mu_z = \mu_0$ in case3; $\varepsilon_t = 2\varepsilon_0$, $\varepsilon_z = 4\varepsilon_0$, $\mu_t = 2\mu_0$, $\mu_z = 2.8\mu_0$ in case4; $\varepsilon_t = (2 + 0.01i)\varepsilon_0$, $\varepsilon_z = (4 + 0.01i)\varepsilon_0$, $\mu_t = (2 + 0.01i)\mu_0$, $\mu_z = (2.8 + 0.01i)\mu_0$ in case5; $\varepsilon_t = 2\varepsilon_0$, $\varepsilon_z = 4\varepsilon_0$, $\mu_t = \mu_z = \mu_0$ in case6, respectively.

Figure 10 shows the effect the incident angle β on the radiation torque. Because the spherical particle is illuminated by an on-axis Gaussian beam, the x and z components of the radiation torques are zero and not plotted in Fig. 10. When the anisotropic sphere is reduced to an isotropic sphere, the radiation torque is invariable and equal to zero in despite of the size of the incident angle (see case1). It can be observed that the negative radiation torque will cause the uniaxial anisotropic to rotate anticlockwise when the incident angle $0 < \beta < 90$; while the positive radiation torque will cause the uniaxial anisotropic to rotate clockwise when the incident angle $90 < \beta < 180$. For the case that the sphere center and the beam center are the same, the distribution radiation torque is symmetrical with $\beta = 90$, and it equals zero when the uniaxial anisotropic sphere is vertically illuminated by a Gaussian beam resulting from the uniaxial anisotropic sphere is symmetrical with x-axis. For the case that $z_0 \neq 0$, namely, the sphere center and beam center are not the same, the radiation torque is not equal to zero(see case6) when the incident angle equals 90 resulting from that the symmetrical axis of the uniaxial anisotropic sphere and the propagation direction of the beam are not the same. It is also can be found that the radiation torque decreases in whole for loss both electrical anisotropic or electrical and magnetic anisotropic sphere compared with those lossless anisotropic sphere. It is different from that performance that the radiation torque changes with the location of the beam center along y-axis shown in Fig. 9.

4. Conclusion

The expansion expressions of an incident Gaussian beam with arbitrary propagation and polarization directions in terms of SVWFs in a fixed coordinate system are derived. The analytical expressions of the Radiation forces and torques exerted on a homogeneous absorbing uniaxial anisotropic sphere are obtained by the incident Gaussian beam. We numerically studied the following: the effects of the anisotropic absorbing dielectric on the variations of axial and transverse components of the RFs exerted on a uniaxial anisotropic sphere, as a function of the center-to-center distance between the beam and sphere; and the variations of the axial, transverse, and resultant RFs with the incident angle and polarization angle exerted by an obliquely Gaussian beam on a uniaxial anisotropic sphere. The numerical results exhibit some interesting phenomena, indicating that the properties of the RF exerted by an obliquely incident Gaussian beam on a uniaxial anisotropic sphere differ from those of the RF exerted on an isotropic sphere. The effects of the location of the beam center and incident angle on the radiation torque exerted on an transparent or absorbing uniaxial anisotropic sphere are numerically analyzed by a linearly polarized Gaussian beam, and the results are compared with those exerted on an isotropic sphere. Due to the length restriction,

#166959 - $15.00 USD Received 18 Apr 2012; revised 8 Jun 2012; accepted 22 Jun 2012; published 5 Jul 2012

the more cases such the effects of the polarization model of the beam, size parameter of the particles and so on are not discussed will be studied in our future work. The developed theory and numerical code presented in this paper serve as useful tools for theoretical and experimental studies on trapping or manipulating uniaxial anisotropic spherical particles. RFs exerted by an arbitrary direction incident Gaussian beam on multiple uniaxial anisotropic spheres will be the subject of future research.

Acknowledgments

The authors gratefully acknowledge support from the National Natural Science Foundation of China under Grant Nos. 61172031 and 60971065 and Fundamental Research Funds for the Central Universities.

#166959 - $15.00 USD Received 18 Apr 2012; revised 8 Jun 2012; accepted 22 Jun 2012; published 5 Jul 2012